Search for Contact Interactions in $e^{\pm}pCollisionsatHERA$

Aaron, F D ; Alexa, C ; Andreev, V ; Backovic, S ; Baghdasaryan, A ; Müller, K ; Robmann, P ; Straumann, U ; Truöl, P

DOI: https://doi.org/10.1016/j.physletb.2011.09.109

DESY 11-114
July 2011

ISSN 0418-9833

Search for Contact Interactions in $e^{\pm}p$ Collisions at HERA

H1 Collaboration

Abstract

A search for physics beyond the Standard Model in neutral current deep inelastic scattering at high negative four-momentum transfer squared Q^2 is performed in $e^{\pm}p$ collisions at HERA. The differential cross section $\mathrm{d}\sigma/\mathrm{d}Q^2$, measured using the full H1 data sample corresponding to an integrated luminosity of 446 pb^{-1}, is compared to the Standard Model prediction. No significant deviation is observed. Limits on various models predicting new phenomena at high Q^2 are derived. For general four-fermion $eeqq$ contact interaction models, lower limits on the compositeness scale Λ are set in the range 3.6 TeV to 7.2 TeV. Leptoquarks with masses M_{LQ} and couplings λ are constrained to $M_{\mathrm{LQ}}/\lambda > 0.41 - 1.86$ TeV and limits on squarks in R-parity violating supersymmetric models are derived. A lower limit on the gravitational scale in (4+n) dimensions of $M_S > 0.9$ TeV is established for low-scale quantum gravity effects in models with large extra dimensions. For the light quark radius an upper bound of $R_q < 0.65 \cdot 10^{-18}$ m is determined.

Submitted to Phys. Lett. **B**

F.D. Aaron[5,48], C. Alexa[5], V. Andreev[25], S. Backovic[30], A. Baghdasaryan[38], S. Baghdasaryan[38], E. Barrelet[29], W. Bartel[11], K. Begzsuren[35], A. Belousov[25], P. Belov[11], J.C. Bizot[27], V. Boudry[28], I. Bozovic-Jelisavcic[2], J. Bracinik[3], G. Brandt[11], M. Brinkmann[11], V. Brisson[27], D. Britzger[11], D. Bruncko[16], A. Bunyatyan[13,38], G. Buschhorn[26,†], L. Bystritskaya[24], A.J. Campbell[11], K.B. Cantun Avila[22], F. Ceccopieri[4], K. Cerny[32], V. Cerny[16,47], V. Chekelian[26], J.G. Contreras[22], J.A. Coughlan[6], J. Cvach[31], J.B. Dainton[18], K. Daum[37,43], B. Delcourt[27], J. Delvax[4], E.A. De Wolf[4], C. Diaconu[21], M. Dobre[12,50,51], V. Dodonov[13], A. Dossanov[26], A. Dubak[30,46], G. Eckerlin[11], S. Egli[36], A. Eliseev[25], E. Elsen[11], L. Favart[4], A. Fedotov[24], R. Felst[11], J. Feltesse[10], J. Ferencei[16], D.-J. Fischer[11], M. Fleischer[11], A. Fomenko[25], E. Gabathuler[18], J. Gayler[11], S. Ghazaryan[11], A. Glazov[11], L. Goerlich[7], N. Gogitidze[25], M. Gouzevitch[11,45], C. Grab[40], A. Grebenyuk[11], T. Greenshaw[18], B.R. Grell[11], G. Grindhammer[26], S. Habib[11], D. Haidt[11], C. Helebrant[11], R.C.W. Henderson[17], E. Hennekemper[15], H. Henschel[39], M. Herbst[15], G. Herrera[23], M. Hildebrandt[36], K.H. Hiller[39], D. Hoffmann[21], R. Horisberger[36], T. Hreus[4,44], F. Huber[14], M. Jacquet[27], X. Janssen[4], L. Jönsson[20], H. Jung[11,4,52], M. Kapichine[9], I.R. Kenyon[3], C. Kiesling[26], M. Klein[18], C. Kleinwort[11], T. Kluge[18], R. Kogler[11], P. Kostka[39], M. Kraemer[11], J. Kretzschmar[18], K. Krüger[15], M.P.J. Landon[19], W. Lange[39], G. Laštovička-Medin[30], P. Laycock[18], A. Lebedev[25], V. Lendermann[15], S. Levonian[11], K. Lipka[11,50], B. List[11], J. List[11], R. Lopez-Fernandez[23], V. Lubimov[24], A. Makankine[9], E. Malinovski[25], P. Marage[4], H.-U. Martyn[1], S.J. Maxfield[18], A. Mehta[18], A.B. Meyer[11], H. Meyer[37], J. Meyer[11], S. Mikocki[7], I. Milcewicz-Mika[7], F. Moreau[28], A. Morozov[9], J.V. Morris[6], M. Mudrinic[2], K. Müller[41], Th. Naumann[39], P.R. Newman[3], C. Niebuhr[11], D. Nikitin[9], G. Nowak[7], K. Nowak[11], J.E. Olsson[11], D. Ozerov[24], P. Pahl[11], V. Palichik[9], I. Panagoulias[l,11,42], M. Pandurovic[2], Th. Papadopoulou[l,11,42], C. Pascaud[27], G.D. Patel[18], E. Perez[10,45], A. Petrukhin[11], I. Picuric[30], S. Piec[11], H. Pirumov[14], D. Pitzl[11], R. Plačakytė[12], B. Pokorny[32], R. Polifka[32], B. Povh[13], V. Radescu[14], N. Raicevic[30], T. Ravdandorj[35], P. Reimer[31], E. Rizvi[19], P. Robmann[41], R. Roosen[4], A. Rostovtsev[24], M. Rotaru[5], J.E. Ruiz Tabasco[22], S. Rusakov[25], D. Šálek[32], D.P.C. Sankey[6], M. Sauter[14], E. Sauvan[21], S. Schmitt[11], L. Schoeffel[10], A. Schöning[14], H.-C. Schultz-Coulon[15], F. Sefkow[11], L.N. Shtarkov[25], S. Shushkevich[26], T. Sloan[17], I. Smiljanic[2], Y. Soloviev[25], P. Sopicki[7], D. South[11], V. Spaskov[9], A. Specka[28], Z. Staykova[4], M. Steder[11], B. Stella[33], G. Stoicea[5], U. Straumann[41], T. Sykora[4,32], P.D. Thompson[3], T.H. Tran[27], D. Traynor[19], P. Truöl[41], I. Tsakov[34], B. Tseepeldorj[35,49], J. Turnau[7], K. Urban[15], A. Valkárová[32], C. Vallée[21], P. Van Mechelen[4], Y. Vazdik[25], D. Wegener[8], E. Wünsch[11], J. Žáček[32], J. Zálešák[31], Z. Zhang[27], A. Zhokin[24], H. Zohrabyan[38], and F. Zomer[27]

[1] *I. Physikalisches Institut der RWTH, Aachen, Germany*
[2] *Vinca Institute of Nuclear Sciences, University of Belgrade, 1100 Belgrade, Serbia*
[3] *School of Physics and Astronomy, University of Birmingham, Birmingham, UK[b]*
[4] *Inter-University Institute for High Energies ULB-VUB, Brussels and Universiteit Antwerpen, Antwerpen, Belgium[c]*
[5] *National Institute for Physics and Nuclear Engineering (NIPNE) , Bucharest, Romania[m]*
[6] *Rutherford Appleton Laboratory, Chilton, Didcot, UK[b]*
[7] *Institute for Nuclear Physics, Cracow, Poland[d]*
[8] *Institut für Physik, TU Dortmund, Dortmund, Germany[a]*
[9] *Joint Institute for Nuclear Research, Dubna, Russia*
[10] *CEA, DSM/Irfu, CE-Saclay, Gif-sur-Yvette, France*

[11] *DESY, Hamburg, Germany*
[12] *Institut für Experimentalphysik, Universität Hamburg, Hamburg, Germany*[a]
[13] *Max-Planck-Institut für Kernphysik, Heidelberg, Germany*
[14] *Physikalisches Institut, Universität Heidelberg, Heidelberg, Germany*[a]
[15] *Kirchhoff-Institut für Physik, Universität Heidelberg, Heidelberg, Germany*[a]
[16] *Institute of Experimental Physics, Slovak Academy of Sciences, Košice, Slovak Republic*[f]
[17] *Department of Physics, University of Lancaster, Lancaster, UK*[b]
[18] *Department of Physics, University of Liverpool, Liverpool, UK*[b]
[19] *Queen Mary and Westfield College, London, UK*[b]
[20] *Physics Department, University of Lund, Lund, Sweden*[g]
[21] *CPPM, Aix-Marseille Université, CNRS/IN2P3, Marseille, France*
[22] *Departamento de Fisica Aplicada, CINVESTAV, Mérida, Yucatán, México*[j]
[23] *Departamento de Fisica, CINVESTAV IPN, México City, México*[j]
[24] *Institute for Theoretical and Experimental Physics, Moscow, Russia*[k]
[25] *Lebedev Physical Institute, Moscow, Russia*[e]
[26] *Max-Planck-Institut für Physik, München, Germany*
[27] *LAL, Université Paris-Sud, CNRS/IN2P3, Orsay, France*
[28] *LLR, Ecole Polytechnique, CNRS/IN2P3, Palaiseau, France*
[29] *LPNHE, Université Pierre et Marie Curie Paris 6, Université Denis Diderot Paris 7, CNRS/IN2P3, Paris, France*
[30] *Faculty of Science, University of Montenegro, Podgorica, Montenegro*[n]
[31] *Institute of Physics, Academy of Sciences of the Czech Republic, Praha, Czech Republic*[h]
[32] *Faculty of Mathematics and Physics, Charles University, Praha, Czech Republic*[h]
[33] *Dipartimento di Fisica Università di Roma Tre and INFN Roma 3, Roma, Italy*
[34] *Institute for Nuclear Research and Nuclear Energy, Sofia, Bulgaria*[e]
[35] *Institute of Physics and Technology of the Mongolian Academy of Sciences, Ulaanbaatar, Mongolia*
[36] *Paul Scherrer Institut, Villigen, Switzerland*
[37] *Fachbereich C, Universität Wuppertal, Wuppertal, Germany*
[38] *Yerevan Physics Institute, Yerevan, Armenia*
[39] *DESY, Zeuthen, Germany*
[40] *Institut für Teilchenphysik, ETH, Zürich, Switzerland*[i]
[41] *Physik-Institut der Universität Zürich, Zürich, Switzerland*[i]

[42] *Also at Physics Department, National Technical University, Zografou Campus, GR-15773 Athens, Greece*
[43] *Also at Rechenzentrum, Universität Wuppertal, Wuppertal, Germany*
[44] *Also at University of P.J. Šafárik, Košice, Slovak Republic*
[45] *Also at CERN, Geneva, Switzerland*
[46] *Also at Max-Planck-Institut für Physik, München, Germany*
[47] *Also at Comenius University, Bratislava, Slovak Republic*
[48] *Also at Faculty of Physics, University of Bucharest, Bucharest, Romania*
[49] *Also at Ulaanbaatar University, Ulaanbaatar, Mongolia*
[50] *Supported by the Initiative and Networking Fund of the Helmholtz Association (HGF) under the contract VH-NG-401.*

[51] *Absent on leave from NIPNE-HH, Bucharest, Romania*
[52] *On leave of absence at CERN, Geneva, Switzerland*

[†] *Deceased*

[a] *Supported by the Bundesministerium für Bildung und Forschung, FRG, under contract numbers 05H09GUF, 05H09VHC, 05H09VHF, 05H16PEA*
[b] *Supported by the UK Science and Technology Facilities Council, and formerly by the UK Particle Physics and Astronomy Research Council*
[c] *Supported by FNRS-FWO-Vlaanderen, IISN-IIKW and IWT and by Interuniversity Attraction Poles Programme, Belgian Science Policy*
[d] *Partially Supported by Polish Ministry of Science and Higher Education, grant DPN/N168/DESY/2009*
[e] *Supported by the Deutsche Forschungsgemeinschaft*
[f] *Supported by VEGA SR grant no. 2/7062/ 27*
[g] *Supported by the Swedish Natural Science Research Council*
[h] *Supported by the Ministry of Education of the Czech Republic under the projects LC527, INGO-LA09042 and MSM0021620859*
[i] *Supported by the Swiss National Science Foundation*
[j] *Supported by CONACYT, México, grant 48778-F*
[k] *Russian Foundation for Basic Research (RFBR), grant no 1329.2008.2*
[l] *This project is co-funded by the European Social Fund (75%) and National Resources (25%) - (EPEAEK II) - PYTHAGORAS II*
[m] *Supported by the Romanian National Authority for Scientific Research under the contract PN 09370101*
[n] *Partially Supported by Ministry of Science of Montenegro, no. 05-1/3-3352*

1 Introduction

Deep inelastic neutral current (NC) scattering $e^{\pm}p \rightarrow e^{\pm}X$ at high negative four-momentum transfer squared Q^2 allows the structure of eq interactions to be probed at short distances and to search for new phenomena beyond the Standard Model (SM). Using the concept of four-fermion contact interactions (CI) the interference of the photon and Z-boson fields with any new particle field associated to larger scales can be investigated.

Results from searches for contact interactions in ep interactions at HERA have been previously reported by the H1 [1, 2] and ZEUS [3, 4] collaborations. Therein, genuine contact interaction models, models with leptoquarks and supersymmetric scalar quarks (squarks), low-scale quantum gravity models with large extra dimensions and compositeness models of quarks have been investigated by searching for deviations from the SM expectation at high Q^2. Contact interaction studies have been also performed at LEP [5].

Such models have also been investigated in direct searches at HERA, the Tevatron and the LHC. Searches for leptoquarks involving lepton flavour violation [6] and squarks in R-parity violating ($\not{R}_p$) supersymmetric models [7] have been published by the H1 collaboration using the full HERA data. Searches for leptoquark pair production in proton-proton collisions at a centre–of–mass energy of $\sqrt{s} = 7$ TeV were reported by the ATLAS [8] and CMS [9] collaborations, excluding first generation scalar leptoquarks up to 376 TeV and 384 TeV, respectively. These results surpass limits obtained at the Tevatron [10]. Stringent limits on low-scale quantum gravity models with large extra dimensions using di-jet, di-electron and di-photon final states have been reported by the DØ collaboration [11, 12] and recently, by the CMS collaboration, excluding mass scales below 1.6-2.3 TeV depending on the model [13].

The analysis in this paper is based on the full H1 data sample collected in the years 1994-2007, which corresponds to an integrated luminosity of $\mathcal{L} = 446$ pb^{-1} and represents a factor of $3(12)$ increase in statistics for e^+p (e^-p) collisions with respect to the previous publications [1]. The same method is used as in previous analysis which is superseded by the results presented in this paper.

2 Contact Interaction Models

New physics phenomena in fermion-fermion scattering experiments may manifest themselves in deviations of the differential cross section $\mathrm{d}\sigma/\mathrm{d}Q^2$ from the SM expectation, and may be related to new heavy particles with masses M_X much larger than the electroweak scale. In the low energy limit $\sqrt{s} \ll M_X$ such phenomena can be described by an effective four-fermion CI model. Different implementations of this effective model are summarised in the following.

2.1 General contact interactions and compositeness

In ep scattering, the most general chiral invariant Lagrangian for neutral current vector-like four-fermion contact interactions can be written in the form [14, 15]:

$$\mathcal{L}_V = \sum_q \sum_{a,\,b\,=\,L,\,R} \eta^q_{ab}\,(\bar{e}_a\gamma_\mu e_a)(\bar{q}_b\gamma^\mu q_b)\,, \tag{1}$$

where η^q_{ab} are the CI coupling coefficients, a and b indicate the left-handed and right-handed fermion helicities and the first sum is over all quark flavours. In the kinematic region of interest mainly the valence quarks (u and d) contribute.

In the case of general models of fermion compositeness or substructure the CI coupling coefficients are defined as:

$$\eta^q_{ab} = \epsilon^q_{ab} \frac{4\pi}{\Lambda^2} \,. \tag{2}$$

New physics models are then characterised by a common compositeness scale Λ and the coefficients ϵ^q_{ab}, which describe the chiral structure of the coupling and may take the values ± 1 or 0, depending on the scenario, for example pure left-handed (L), right-handed (R), or vector (V) and axial-vector (A) couplings. Depending on the model and the sign of the coefficients, the new physics processes interfere either constructively or destructively with the SM processes.

2.2 Leptoquarks

Leptoquarks, colour triplet scalar or vector bosons carrying lepton and baryon number, appear naturally in extensions of the SM which aim to unify the lepton and quark sectors. For leptoquark masses M_{LQ} much larger than the probing scale $M_{\mathrm{LQ}} \gg \sqrt{s}$, the coupling λ is related to the CI coupling coefficients via:

$$\eta^q_{ab} = \epsilon^q_{ab} \frac{\lambda^2}{M^2_{\mathrm{LQ}}} \,. \tag{3}$$

The classification of the leptoquarks follows the Buchmüller-Rückl-Wyler (BRW) model [16], in which the coefficients ϵ^q_{ab} depend on the leptoquark type [17] and take values 0, $\pm\frac{1}{2}$, ± 1, ± 2.

Two leptoquark types, S^L_0 and $\tilde{S}^L_{1/2}$, have quantum numbers identical to the squarks $\tilde{d}$ and $\tilde{u}$. For these leptoquarks the couplings λ correspond to the Yukawa couplings, λ'_{ijk}, which describe the $R\!\!\!/_p$ supersymmetric $L_i Q_j \bar{D}_k$ interaction [18]. Here i, j and k are the family indices and L_i, Q_j and $\bar{D}_k$ are the super-fields containing the left-handed leptons, the left-handed up-type quarks and the right-handed down-type quarks, respectively, together with their supersymmetric partners.

2.3 Large extra dimensions

In some string inspired models the small nature of the gravitational force is explained by the existence of compactified extra dimensions [19]. In these models the gravitational scale M_S in $4+n$ dimensions is related to the size R of the compactified extra dimensions via the Planck scale $M_P^2 \sim R^n M_S^{2+n}$. SM particles reside on a four-dimensional brane, while the spin 2 graviton propagates into the extra spatial dimensions creating a tower of Kaluza-Klein states. Assuming that the ultraviolet cut-off scale of the tower is of similar size to the gravitational scale, an effective contact-type interaction [20] term can be defined with a coupling coefficient:

$$\eta_G = \frac{\lambda}{M_S^4} \,. \tag{4}$$

The coupling λ depends on details of the theory and is conventionally set to ± 1.

2.4 Quark Radius

A clear manifestation of substructure would be the observation of finite size effects like the measurement of electroweak charge distributions of fermions. Finite size effects are typically described by a standard form factor in the eq scattering cross section:

$$f(Q^2) \;=\; 1 - \frac{\langle R^2 \rangle}{6} Q^2 \,, \tag{5}$$

which relates the decrease of the scattering cross sections at high Q^2 to the mean squared radius $\langle R^2 \rangle$ of the electroweak charge distribution. This form factor modifies the Q^2 dependence of the ep scattering cross section similarly to the CI models described above.

3 Data and Analysis Method

The analysed data sample is recorded in e^+p and e^-p collisions corresponding to an integrated luminosity of 281 pb^{-1} and 165 pb^{-1}, respectively. The measurement of the differential neutral current cross-section, $\mathrm{d}\sigma/\mathrm{d}Q^2$, which is used to probe possible CI signatures follows the previous measurements based on data recorded in the years 1994-2000 [21–23] and includes new data recorded from 2003-2007. A list of the analysed data sets is given in table 1.

Reaction	$\mathcal{L}_{int}$ [pb^{-1}]	$\sqrt{s}$ [GeV]	Polarisation (P_e [%])
$e^+p \to e^+X$	36	301	Unpolarised
$e^-p \to e^-X$	16	319	Unpolarised
$e^+p \to e^+X$	65	319	Unpolarised
$e^-p \to e^-X$	46	319	Right $(P_e = +37)$
$e^-p \to e^-X$	103	319	Left $(P_e = -26)$
$e^+p \to e^+X$	98	319	Right $(P_e = +33)$
$e^+p \to e^+X$	82	319	Left $(P_e = -38)$

Table 1: Data samples recorded in the years 1994-2007 with corresponding integrated luminosities, centre-of-mass energies and average longitudinal polarisations.

The data collected from the year 2003 onwards were taken with a longitudinally polarised lepton beam, with typical polarisation values of $\pm 35\%$. The average luminosity weighted polarisations of the e^+p and e^-p data sets are small. Due to the different chiral structure of hypothetical new particles with respect to the irreducible SM background, the sensitivity to possible new physics phenomena is increased by up to 15 percent by analysing the data sets with left and right longitudinal lepton polarisation separately.

Contact interactions are investigated by searching for deviations in the NC differential cross section $\mathrm{d}\sigma/\mathrm{d}Q^2$ from the SM expectation at high negative four-momentum transfer squared $Q^2 > 200$ GeV^2. The SM cross section of neutral current scattering factorises into the electroweak matrix element of the hard eq interaction process and the parton distribution function (PDF) of the proton. The Q^2 dependence of the PDF is calculated using perturbative QCD [24].

For the CI analysis the parton densities at high values of Q^2, corresponding to high values of x, are of special importance. In this analysis the CTEQ6m [25] PDF is used to calculate both the SM and signal expectations. The CTEQ6m set was obtained by fitting several experimental data sets. At high x this PDF is mostly constrained by fixed target experiments and also by W-boson production and jet data from the Tevatron experiments, which are not sensitive to possible eq contact interaction processes. CTEQ6m also includes early $e^{\pm}p$ scattering data at high Q^2 from the H1 ($\mathcal{L} = 52$ pb^{-1}) and ZEUS ($\mathcal{L} = 30$ pb^{-1}) experiments. However, since the e^+p (e^-p) data sets analysed here are $6(10)$ times larger, the residual correlations between the HERA data and the CTEQ6m PDF are small and are neglected in the following. Furthermore, the CTEQ6m parton densities can be regarded as unbiased with respect to possible contact interaction effects. CTEQ6m is chosen as it describes many experimental data and in particular, the HERA data in the region $Q^2 < 200$ GeV^2, which are not used in this analysis. The results of this analysis are verified using an alternative PDF not based on HERA high Q^2 data, as described in section 4.

The single differential cross sections $\mathrm{d}\sigma/\mathrm{d}Q^2$ are measured for e^+p and e^-p scattering up to $Q^2 = 30000$ GeV^2 and compared to the SM expectation. The ratio of the data to the SM expectation is shown in figure 1. Good agreement between data and the SM is observed, in particular in the high Q^2 region, which is the focus of this analysis.

In the next step, a quantitative test of the SM and the CI models is performed by investigating the measured cross sections $\mathrm{d}\sigma/\mathrm{d}Q^2$ following the analysis method described in [1] by applying a minimisation of the χ^2 function [26]:

$$\chi^2(\eta,\varepsilon) = \sum_i \frac{\left(\sigma_i^{\mathrm{exp}} - \sigma_i^{\mathrm{th}}(\eta)\left(1-\sum_k \Delta_{ik}(\varepsilon_k)\right)\right)^2}{\delta_{i,\mathrm{stat}}^2\,\sigma_i^{\mathrm{exp}}\sigma_i^{\mathrm{th}}(\eta)\left(1-\sum_k \Delta_{ik}(\varepsilon_k)\right) + \left(\delta_{i,\mathrm{uncor}}\,\sigma_i^{\mathrm{exp}}\right)^2} + \sum_k \varepsilon_k^2\,. \qquad (6)$$

Here σ_i^{exp} and $\sigma_i^{\mathrm{th}}(\eta)$ are the experimental and theoretical cross sections, respectively, for the measurement point i, and $\delta_{i,\mathrm{stat}}$ and $\delta_{i,\mathrm{uncor}}$ correspond to the relative statistical and uncorrelated systematic errors, respectively. The theoretical cross section includes both the SM and the contact interaction term, and it depends on the coupling coefficient η, which is varied in the fit. The functions $\Delta_{ik}(\varepsilon_k)$ describe the correlated systematic errors for point i associated to a source k and depend on the fit parameters ε_k. In particular, the normalisations of the individual data sets described in table 1 are free parameters, only constrained by the individual luminosity measurements. Since the precise cross section measurements at low Q^2 determine the normalisations, new physics signals are mainly tested by exploiting the shape of the Q^2 distribution.

Statistical and systematic uncertainties are taken into account in the fit procedure. The following sources of experimental uncertainties are accounted for [21–23, 27]: the electromagnetic energy scale uncertainty of $1-3\%$, the polar angle uncertainty of the scattered lepton of $2-3$ mrad, the uncertainty on the electron identification of $0.5-2\%$, the hadronic energy scale uncertainty of $2-7\%$ the uncertainty from the luminosity measurement of $1.6-3.8\%$ and the uncertainty on the electron beam polarisation of $1-2.3\%$. The effect of the above systematic uncertainties on the SM expectation is determined by varying the experimental quantities by ± 1 standard deviation in the MC samples and propagating these variations through the whole analysis. The uncorrelated systematic uncertainties of the measurements vary as function of Q^2 between $1-11\%$ $(1.6-13\%)$ for e^+p (e^-p) scattering. The dominant sources of the correlated systematic errors are the PDF uncertainty (about 8%), the uncertainties from the luminosity

measurement and from the experimental uncertainties on the energy scale and the polar angle of the scattered lepton. All other experimental systematic uncertainties are found to have a negligible impact on the analysis.

4 Results

The data used in this analysis are found to be consistent with the expectation from the SM alone ($\eta = 0$ in equation 6) based on the CTEQ6m PDF, yielding a $\chi^2/dof = 16.4/17$ $(7.0/17)$ for the e^+p (e^-p) data. The normalisation constants of the individual data sets agree well with the SM expectation within the PDF uncertainties.

For each CI model the effective scale parameters and couplings describing the new physics scale are determined by a fit to the differential NC cross section. All scale parameters are found to be consistent with the SM and limits are calculated at 95% confidence levels (CL) using the frequentist method as described in the previous publication [1].

Lower limits on the compositeness scale Λ in the context of the general contact interaction model are presented in table 2 and figure 2. The results are presented for eight scenarios, which differ in their chiral structure as determined by the CI coupling coefficients η^q_{ab}. Depending on the model and the sign of the coefficients, limits on Λ are obtained in the range 3.6 TeV to 7.2 TeV. In figure 3, differential cross section measurements for e^+p and e^-p scattering normalised to the SM expectation are compared to the predictions corresponding to the 95% CL exclusion limits of the VV model, $\Lambda^+_{VV} > 5.6$ TeV and $\Lambda^-_{VV} > 7.2$ TeV.

For leptoquark-type contact interactions, the notation, quantum numbers and lower limits on M_{LQ}/λ are presented in table 3. The limits are in the range $M_{\mathrm{LQ}}/\lambda > 0.41 - 1.86$ TeV. Leptoquarks coupling to u quarks are probed with higher sensitivity, corresponding to more stringent limits than those coupling to d quarks due to the different quark densities in the proton. In figure 4, the normalised differential $e^\pm p$ cross section measurements are compared to the predicted cross sections corresponding to the 95% CL exclusion limits of the S^L_1 and V^L_1 leptoquarks. At high Q^2 the existence of a S^L_1 (V^L_1) leptoquark would lead to an increase (decrease) of the $e^\pm p$ cross sections, which is not observed. For a Yukawa coupling of electromagnetic strength, $\lambda = 0.3$, scalar and vector leptoquark masses up to 0.33 TeV and 0.56 TeV are excluded, respectively, comparable or exceeding limits obtained by Tevatron and LHC. The leptoquarks S^L_0 and $\tilde{S}^L_{1/2}$ may also be interpreted as squarks in the framework of $R\!\!\!/_p$ supersymmetry and the corresponding limits in terms of the ratio $M_{\tilde{q}}/\lambda'$ are given in table 4. For a Yukawa coupling of electromagnetic strength, the corresponding lower limit on the $\tilde{u}$ mass of 0.33 TeV is similar to that obtained recently by the H1 collaboration in a direct search [7].

Lower limits in a model with large extra dimensions on the gravitational scale M_S in $4{+}n$ dimensions assuming a positive ($\lambda = +1$) or negative ($\lambda = -1$) coupling are given in table 5. Mass scales $M_S < 0.9$ GeV are excluded at 95% CL. The corresponding cross section predictions normalised to the SM expectation are compared to the $e^\pm p$ data in figure 5.

Finally, an upper limit at 95% CL on the quark radius $R_q < 0.65 \cdot 10^{-18}$ m is derived assuming point-like leptons. The corresponding cross section predictions normalised to the SM expectation are compared to the $e^\pm p$ data in figure 6.

The above results are also verified using a dedicated H1 PDF set based on data collected in the years 1994-2007. This PDF set was obtained from a next-to-leading order QCD fit to the H1 data [26] with $Q^2 < 200$ GeV^2, excluding the high Q^2 data used in this analysis. Both the SM expectation and limits derived using the dedicated H1 PDF agree well with those obtained using the CTEQ6m PDF within the uncertainties.

5 Summary

Neutral current deep inelastic e^-p and e^+p scattering cross section measurements are analysed to search for new phenomena mediated via contact interactions. The data are well described by the Standard Model expectations. Limits on the parameters of various contact interaction models are presented at 95% CL.

Lower limits on the compositeness scale Λ are derived within a general contact interaction analysis. The limits range between 3.6 TeV and 7.2 TeV depending on the chiral structure, corresponding to an increase by a factor of about two compared to previous HERA searches. The study of leptoquark exchange yields lower limits on the ratio M_{LQ}/λ between 0.41 TeV and 1.86 TeV, considerably improving constraints from the previous analysis. Squarks in the framework of R-parity violating supersymmetry with masses satisfying $M_{\tilde{u}}/\lambda'_{1j1} < 1.10$ TeV and $M_{\tilde{d}}/\lambda'_{11k} < 0.66$ TeV are excluded. Possible effects of low-scale quantum gravity with gravitons propagating into extra spatial dimensions are also investigated, where lower limits on the gravitational scale in $4+n$ dimensions $M_S > 0.9$ TeV are found. Finally, a form factor approach yields an upper limit on the size of light u and d quarks of $R_q < 0.65 \cdot 10^{-18}$ m, assuming point-like leptons.

Using the full HERA data set, limits derived in this analysis are more stringent than previous results by H1 and ZEUS. The results can also be compared to those obtained by the LEP, Tevatron and, most recently, LHC collaborations. For most models with Yukawa couplings of electromagnetic strength, or stronger, the analysis presented here provides the most stringent limits on first generation leptoquarks.

Acknowledgements

We are grateful to the HERA machine group whose outstanding efforts have made this experiment possible. We thank the engineers and technicians for their work in constructing and maintaining the H1 detector, our funding agencies for financial support, the DESY technical staff for continual assistance and the DESY directorate for support and for the hospitality which they extend to the non-DESY members of the collaboration.

References

[1] C. Adloff *et al.* [H1 Collaboration], Phys. Lett. B **568** (2003) 35 [hep-ex/0305015].

[2] C. Adloff *et al.* [H1 Collaboration], Phys. Lett. B **479** (2000) 358 [hep-ex/0003002].

[3] S. Chekanov *et al.* [ZEUS Collaboration], Phys. Lett. B **591** (2004) 23 [hep-ex/0401009].

[4] J. Breitweg *et al.* [ZEUS Collaboration], Eur. Phys. J. C **14** (2000) 239 [hep-ex/9905039].

[5] K. Cheung, Phys. Lett. B **517** (2001) 167 [hep-ph/0106251].

[6] F. D. Aaron *et al.* [H1 Collaboration], accepted by Phys. Lett. B [arXiv:1103.4938].

[7] F. D. Aaron *et al.* [H1 Collaboration], Eur. Phys. J. C **71** (2011) 1572 [arXiv:1011.6359].

[8] G. Aad *et al.* [ATLAS Collaboration], submitted to Phys. Rev. D [arXiv:1104.4481].

[9] V. Khachatryan *et al.* [CMS Collaboration], submitted to Phys. Rev. D [arXiv:1012.4031].

[10] V. Abazov *et al.* [DØ Collaboration] Phys. Lett. B **671** (2009) 224 [arXiv:0907.1048].

[11] V. M. Abazov *et al.* [DØ Collaboration], Phys. Rev. Lett. **102** (2009) 051601 [arXiv:0809.2813].

[12] V. M. Abazov *et al.* [DØ Collaboration], Phys. Rev. Lett. **103** (2009) 191803 [arXiv:0906.4819].

[13] S. Chatrchyan *et al.* [CMS Collaboration], JHEP **1105** (2011) 085 [arXiv:1103.4279].

[14] E. Eichten, K. D. Lane and M. E. Peskin, Phys. Rev. Lett. **50** (1983) 811;
R. Rückl, Phys. Lett. B **129** (1983) 363;
R. Rückl, Nucl. Phys. B **234** (1984) 91.

[15] P. Haberl, F. Schrempp and H.-U. Martyn, Proc. Workshop 'Physics at HERA', eds. W. Buchmüller and G. Ingelman, DESY, Hamburg (1991), vol. 2, p. 1133.

[16] W. Buchmüller, R. Rückl and D. Wyler, Phys. Lett. B **191** (1987) 422 [Erratum-ibid. B **448** (1999) 320].

[17] J. Kalinowski, R. Rückl, H. Spiesberger and P. M. Zerwas, Z. Phys. C **74** (1997) 595 [hep-ph/9703288].

[18] J. Butterworth and H. Dreiner, Nucl. Phys. B **397** (1993) 3 [hep-ph/9211204].

[19] N. Arkani-Hamed, S. Dimopoulos and G. R. Dvali, Phys. Lett. B **429** (1998) 263 [hep-ph/9803315];
N. Arkani-Hamed, S. Dimopoulos and G. R. Dvali, Phys. Rev. D **59** (1999) 086004 [hep-ph/9807344].

[20] G. F. Giudice, R. Rattazzi and J. D. Wells, Nucl. Phys. B **544** (1999) 3 [corrections in hep-ph/9811291 v2].

[21] C. Adloff *et al.* [H1 Collaboration], Eur. Phys. J. C **13** (2000) 609 [hep-ex/9908059].

[22] C. Adloff *et al.* [H1 Collaboration], Eur. Phys. J. C **19** (2001) 269 [hep-ex/0012052].

[23] C. Adloff *et al.* [H1 Collaboration], Eur. Phys. J. C **30** (2003) 1 [hep-ex/0304003].

[24] V. N. Gribov and L. N. Lipatov, Sov. J. Nucl. Phys. **15** (1972) 438;
V. N. Gribov and L. N. Lipatov, Sov. J. Nucl. Phys. **15** (1972) 675;
L. N. Lipatov, Sov. J. Nucl. Phys. **20** (1975) 94;
Y. L. Dokshitzer, Sov. Phys. JETP **46** (1977) 641;
G. Altarelli and G. Parisi, Nucl. Phys. B **126** (1977) 298.

[25] J. Pumplin *et al.*, JHEP **0207** (2002) 012 [hep-ph/0201195].

[26] F. D. Aaron *et al.* [H1 Collaboration], Eur. Phys. J. C **63** (2009) 625 [arXiv:0904.0929].

[27] R. Plačakytė, "First Measurement of Charged Current Cross Sections with Longitudinally Polarized Positions at HERA", PhD thesis, University Munich (2006), DESY-THESIS-2006-006 (available at http://www-h1.desy.de/publications/theses list.html);
T.H. Tran, "Precision measurements of the charged and neutral current processes at high Q2 at HERA with polarized electron beam", PhD thesis, University Paris-Sud (2010), LAL-10-28.

H1 Search for General Compositeness			
	$\eta^q_{ab} = \epsilon^q_{ab}\, 4\pi/\Lambda^2$		
Model	[ϵ_{LL}, ϵ_{LR}, ϵ_{RL}, ϵ_{RR}]	Λ^+ [TeV]	Λ^- [TeV]
LL	[±1, 0, 0, 0]	4.2	4.0
LR	[0, ±1, 0, 0]	4.8	3.7
RL	[0, 0, ±1, 0]	4.8	3.8
RR	[0, 0, 0, ±1]	4.4	3.9
VV	[±1, ±1, ±1, ±1]	5.6	7.2
AA	[±1, ∓1, ∓1, ±1]	4.4	5.1
VA	[±1, ∓1, ±1, ∓1]	3.8	3.6
$LL + RR$	[±1, 0, 0, ±1]	5.3	5.1
$LR + RL$	[0, ±1, ±1, 0]	5.4	4.8

Table 2: Lower limits at 95% CL on the compositeness scale Λ. The Λ^+ limits correspond to the upper signs and the Λ^- limits correspond to the lower signs of the chiral coefficients $[\epsilon^q_{LL}, \epsilon^q_{LR}, \epsilon^q_{RL}, \epsilon^q_{RR}]$.

H1 Search for Heavy Leptoquarks				
	$\eta^q_{ab} = \epsilon^q_{ab}\ \lambda^2/M^2_{\rm LQ}$			
LQ	ϵ^u_{ab}	ϵ^d_{ab}	F	$M_{\rm LQ}/\lambda$ [TeV]
S_0^L	$\epsilon^u_{LL} = +\frac{1}{2}$		2	1.10
S_0^R	$\epsilon^u_{RR} = +\frac{1}{2}$		2	1.10
$\tilde{S}_0^R$		$\epsilon^d_{RR} = +\frac{1}{2}$	2	0.41
$S_{1/2}^L$	$\epsilon^u_{LR} = -\frac{1}{2}$		0	0.87
$S_{1/2}^R$	$\epsilon^u_{RL} = -\frac{1}{2}$	$\epsilon^d_{RL} = -\frac{1}{2}$	0	0.59
$\tilde{S}_{1/2}^L$		$\epsilon^d_{LR} = -\frac{1}{2}$	0	0.66
S_1^L	$\epsilon^u_{LL} = +\frac{1}{2}$	$\epsilon^d_{LL} = +1$	2	0.71
V_0^L		$\epsilon^d_{LL} = -1$	0	1.06
V_0^R		$\epsilon^d_{RR} = -1$	0	0.91
$\tilde{V}_0^R$	$\epsilon^u_{RR} = -1$		0	1.35
$V_{1/2}^L$		$\epsilon^d_{LR} = +1$	2	0.51
$V_{1/2}^R$	$\epsilon^u_{RL} = +1$	$\epsilon^d_{RL} = +1$	2	1.44
$\tilde{V}_{1/2}^L$	$\epsilon^u_{LR} = +1$		2	1.58
V_1^L	$\epsilon^u_{LL} = -2$	$\epsilon^d_{LL} = -1$	0	1.86

Table 3: Lower limits at 95% CL on $M_{\rm LQ}/\lambda$ for scalar (S) and vector (V) leptoquarks, where L and R denote the lepton chirality and the subscript ($0,\ 1/2,\ 1$) is the weak isospin. For each leptoquark type, the relevant coefficients ϵ^q_{ab} and fermion number $F = L + 3B$ are indicated. Leptoquarks with identical quantum numbers except for weak hypercharge are distinguished using a tilde, for example V_0^R and $\tilde{V}_0^R$. Quantum numbers and helicities refer to $e^- q$ and $e^- \bar{q}$ states.

H1 Search for $\not{R}_p$ Squarks			
Channel	Coupling	ϵ^q_{ab}	$M_{\tilde{q}}/\lambda'$ [TeV]
$e^+ d \to \tilde{u}^{\,(k)}$	λ'_{11k}	$\epsilon^u_{LL} = +\frac{1}{2}$	1.10
$e^- u \to \tilde{d}^{\,(j)}$	λ'_{1j1}	$\epsilon^d_{LR} = -\frac{1}{2}$	0.66

Table 4: Lower limits at 95% CL on $M_{\tilde{q}}/\lambda'$ for the R_p violating couplings λ'_{ijk} [18], where i, j, k are family indices. The coefficients ϵ^q_{ab} are also shown. The λ'_{11k} (λ'_{1j1}) coupling corresponds to the S_0^L ($\tilde{S}_{1/2}^L$) leptoquark coupling shown in table 3.

H1 Search for Large Extra Dimensions	
$\eta_G = \lambda/M_S^4$	
coupling λ	M_S [TeV]
$+1$	0.90
-1	0.92

Table 5: Lower limits at 95% CL on a model with large extra dimensions on the gravitational scale M_S in $4 + n$ dimensions, assuming positive ($\lambda = +1$) or negative ($\lambda = -1$) couplings.

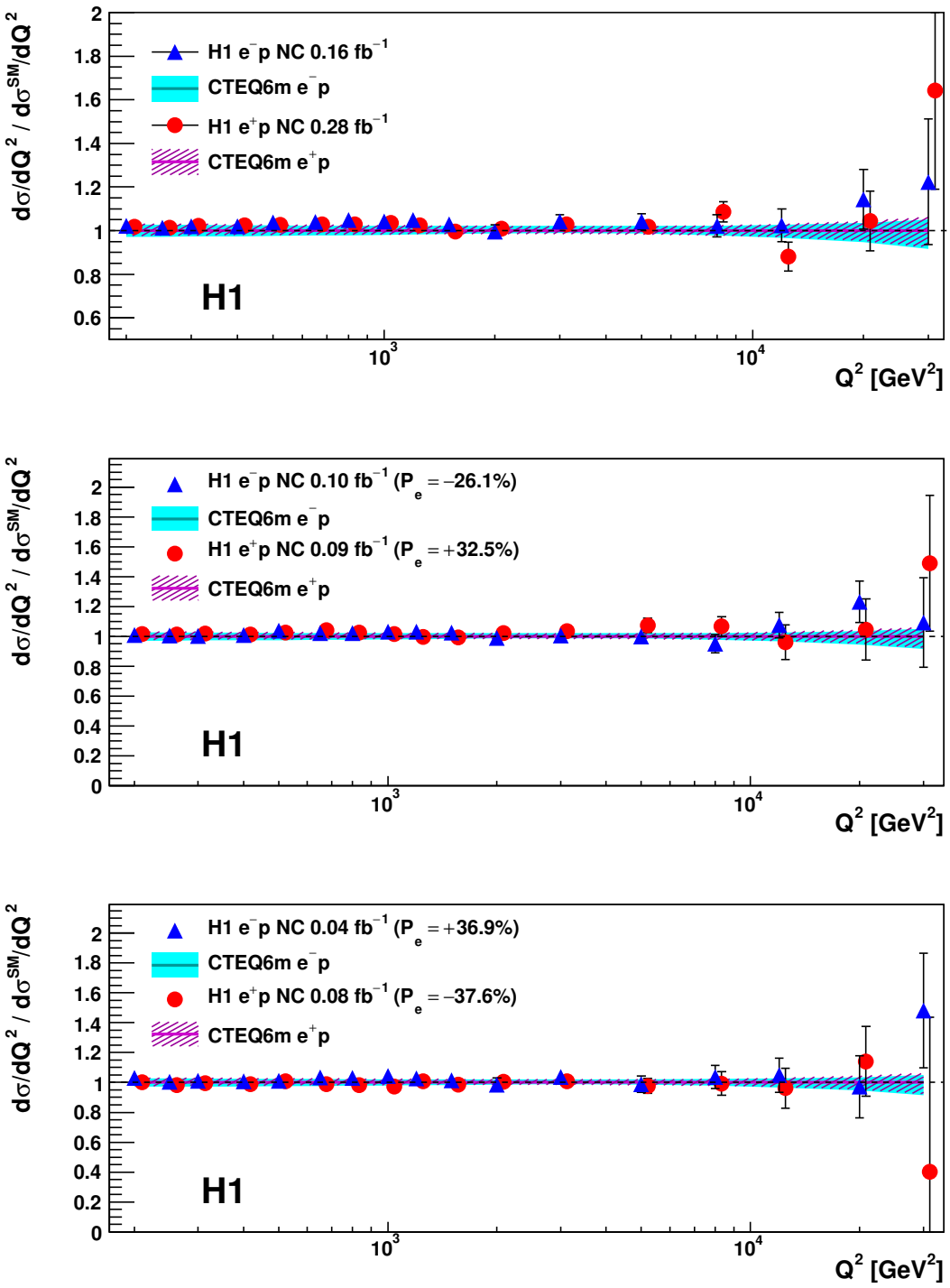

Figure 1: The ratio of the measured cross section to the Standard Model prediction determined using the CTEQ6m PDF set for $e^+p \to e^+X$ and $e^-p \to e^-X$ scattering. The top figurecorresponds to the full H1 data with an average longitudinal polarisation of $P \approx 0$. The middle and bottom figuresrepresent polarised H1 data taken from the year 2003 onwards for different lepton charge and polarisation data sets. The error bars represent the statistical and uncorrelated systematic errors added in quadrature. The bands indicate the PDF uncertainties of the Standard Model cross section predictions.

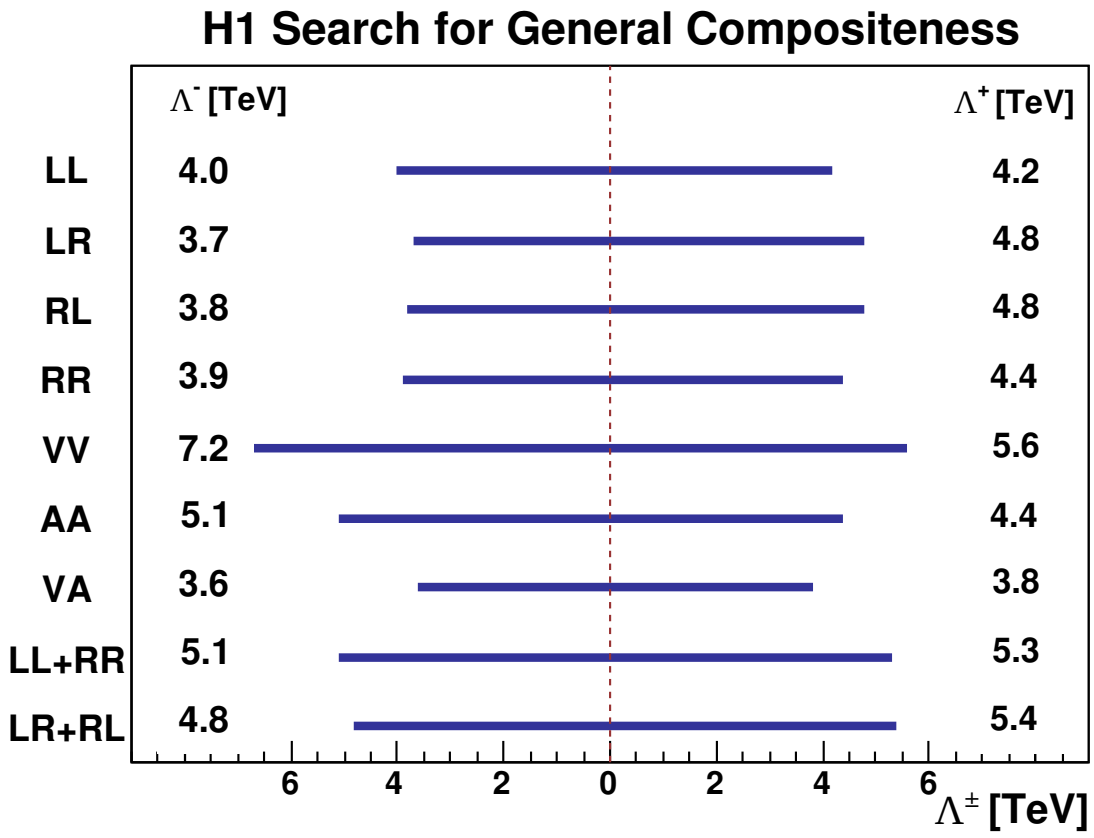

Figure 2: Lower limits at 95% CL on the compositeness scale Λ for various chiral models, obtained from the full H1 data. Limits are given for both signs Λ^+ and Λ^- of the chiral coefficients.

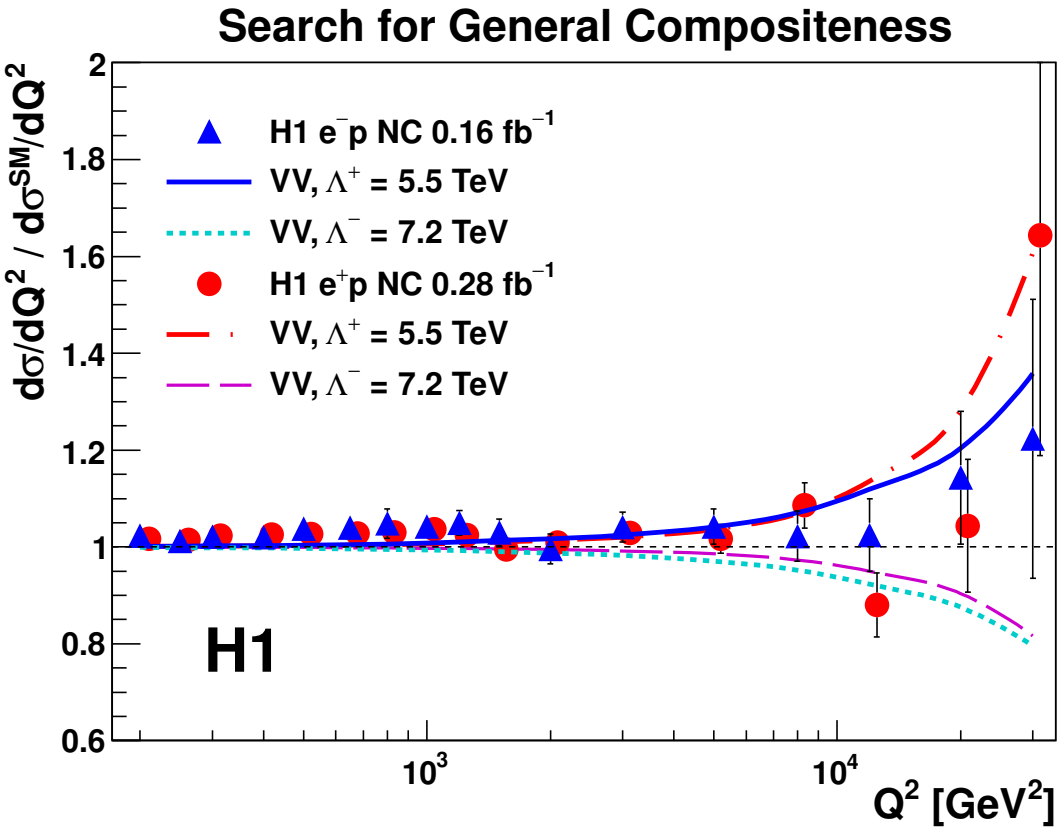

Figure 3: The measured neutral current cross section $\mathrm{d}\sigma/\mathrm{d}Q^2$ normalised to the Standard Model expectation. H1 $e^{\pm}p$ scattering data are compared with curves corresponding to 95% CL exclusion limits obtained from the full H1 data for the VV compositeness scale model, for both signs Λ^+ and Λ^- of the chiral coefficients. The error bars represent the statistical and uncorrelated systematic errors added in quadrature.

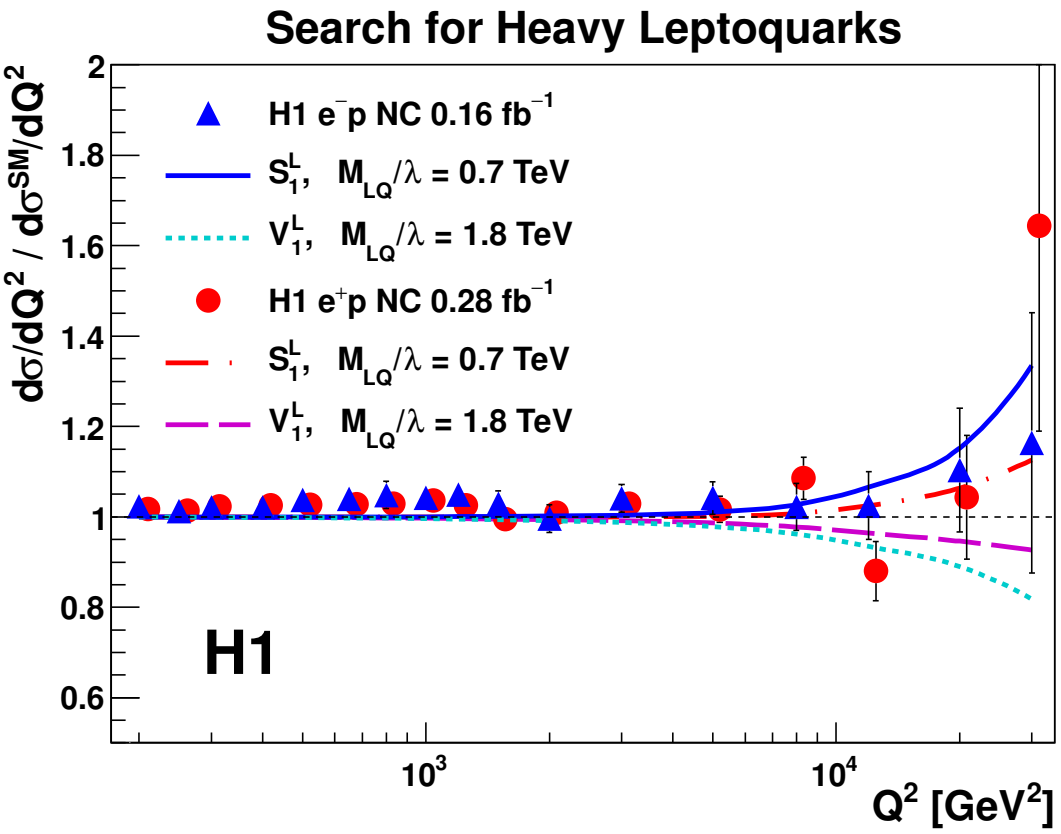

Figure 4: The measured neutral current cross section $\mathrm{d}\sigma/\mathrm{d}Q^2$ normalised to the Standard Model expectation. H1 $e^{\pm}p$ scattering data are compared with curves corresponding to 95% CL exclusion limits obtained from the full H1 data on the ratio M_{LQ}/λ for the S_1^L and V_1^L leptoquarks. The error bars represent the statistical and uncorrelated systematic errors added in quadrature.

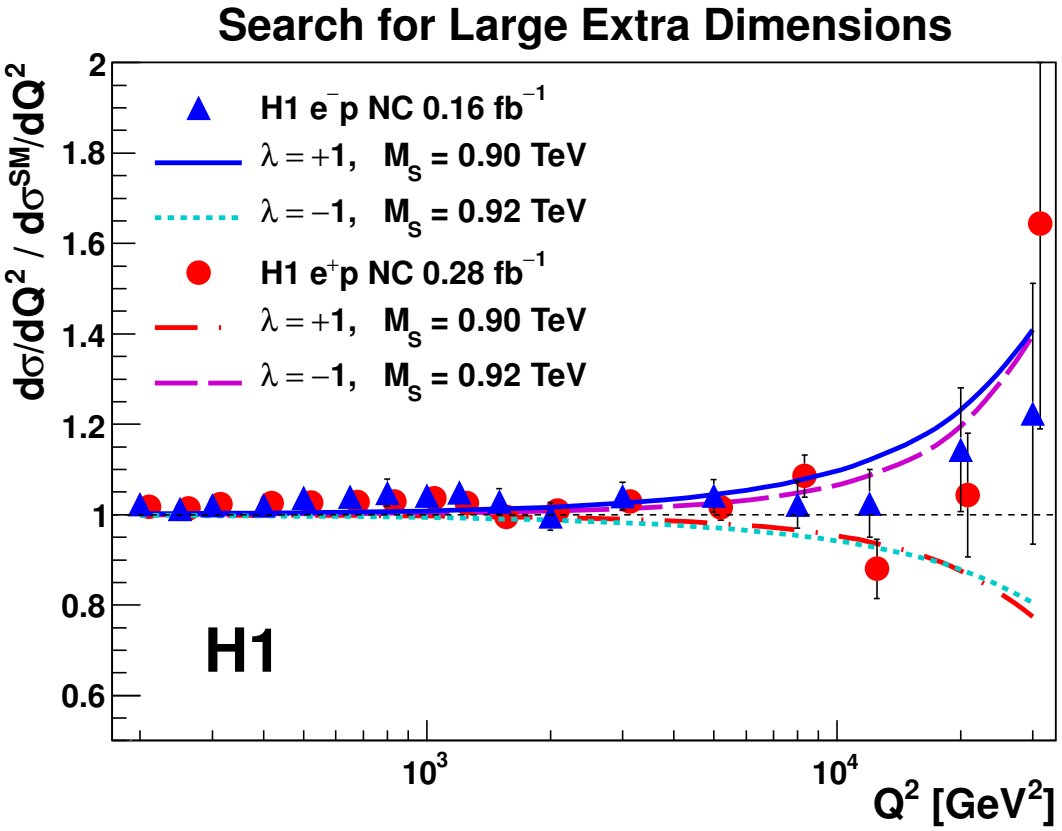

Figure 5: The measured neutral current cross section $\mathrm{d}\sigma/\mathrm{d}Q^2$ normalised to the Standard Model expectation. H1 $e^{\pm}p$ scattering data are compared with curves corresponding to 95% CL exclusion limits obtained from the full H1 data on the gravitational scale, M_S for both positive ($\lambda = +1$) and negative ($\lambda = -1$) couplings. The error bars represent the statistical and uncorrelated systematic errors added in quadrature.

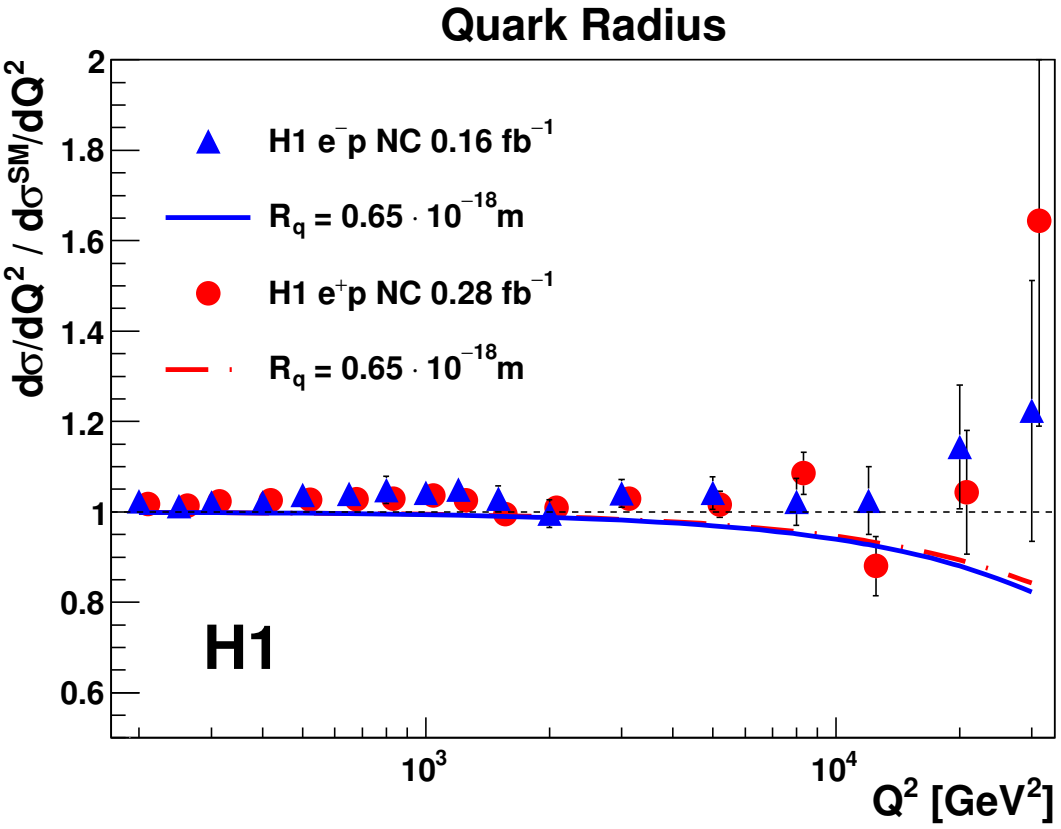

Figure 6: The measured neutral current cross section $\mathrm{d}\sigma/\mathrm{d}Q^2$ normalised to the Standard Model expectation. H1 $e^{\pm}p$ scattering data are compared with curves corresponding to 95% CL exclusion limits obtained from the full H1 data on the quark radius, R_q assuming point-like leptons. The error bars represent the statistical and uncorrelated systematic errors added in quadrature.